RC25189 (W1107-047) July 14, 2011
Physics

IBM Research Report

Microwave-Controlled Universal Entangling Gate for Fixed-Frequency Superconducting Qubits

Jerry M. Chow[1], A. D. Corcoles[1], Jay M. Gambetta[1], Chad Rigetti[1], B. R. Johnson[2], John A. Smolin[1], J. R. Rozen[1], George A. Keefe[1], Mary E. Rothwell[1], Mark Ketchen[1], M. Steffen[1]

[1]IBM Research Division
Thomas J. Watson Research Center
P.O. Box 218
Yorktown Heights, NY 10598

[2]Raytheon BBN Technologies
Cambridge, MA 02138

Research Division
Almaden - Austin - Beijing - Cambridge - Haifa - India - T. J. Watson - Tokyo - Zurich

Microwave-controlled universal entangling gate for fixed-frequency superconducting qubits

Jerry M. Chow,[1] A. D. Córcoles,[1] Jay M. Gambetta,[1] Chad Rigetti,[1] B. R. Johnson,[2] John A. Smolin,[1] J. R. Rozen,[1] George A. Keefe,[1] Mary B. Rothwell,[1] Mark Ketchen,[1] and M. Steffen[1]

[1]*IBM T.J. Watson Research Center, Yorktown Heights, NY 10598, USA*
[2]*Raytheon BBN Technologies, Cambridge, MA 02138, USA*

(Dated: 9th May 2011)

A basic requirement for fault tolerant quantum computing is a universal set of nearly perfect single- and two-qubit gates. As high-fidelity single-qubit operations on superconducting qubits become routine[1,2], the focus shifts onto developing robust and scaleable two-qubit gates. Already, rapid progress has been made, including a controlled-NOT gate with fixed coupled qubits[3], and highly entangled states of two[4,5] and three[6,7] qubits generated from tuning the qubits to explicit resonance conditions. However, as superconducting systems scale up, fixed-coupled systems become difficult to individually address, and tuning to resonances in a spectrally crowded frequency space is problematic. Here we demonstrate a new microwave controlled two-qubit gate[8–10] on capacitively-shunted flux qubits[11] parked at locations of optimal coherence and coupled via a quantum bus. The effective interaction is tunable via irradiation of one qubit at the other qubit's transition frequency. We use this cross-resonance (CR) gate to generate Bell states with a maximal fidelity of 90% and concurrence of 0.88, limited by qubit relaxation. Quantum process tomography gives a gate fidelity of 81%. This gate scheme is readily extendable to systems of more than two qubits and would permit coupling of qubits which are non-nearest neighbours in frequency.

Controlling the effective interaction between qubits is a critical aspect for scaling up quantum computing architectures. This control can be achieved by either 1) tuning the coupling energy between the qubits; or 2) dynamically changing the detuning between qubits in the presence of some small fixed coupling. In the first case, the coupling takes the form of a non-linear tunable subcircuit which can be driven with either microwaves[12–14] or dc[15,16]. This scheme has the benefit of allowing the qubits to be operated at their optimal bias points for coherence. However, the additional control lines for the tunable subcircuit can also result in added circuit complexity over the minimal set of controls necessary for manipulating the qubits. In the second case, which requires no additional controls other than those for the qubits, two-qubit gates have been demonstrated such as square root of i-SWAP[17,18] by tuning the qubit energy levels into resonance, and conditional phase[4] by tuning into a resonance condition involving higher energy levels of the qubits. Although this scheme has been effective for systems up to three qubits[6,7], tuning qubit frequencies in devices with even more qubits could lead to unwanted coupling to noncomputational energy levels of the system and to spurious modes of the electromagnetic environment. Hence, desiderata for a scaleable qubit coupling would combine the tunability of the effective coupling strength with the simplicity of fixed coupling, in an architecture amenable to a larger number of qubits.

Here we report on a new two-qubit gate which combines the hardware simplicity of a fixed coupling scheme with a tunable effective interaction enacted with only microwave control, all on a quantum bus architecture[19,20]. The circuit QED architecture is befitting for testing our gate protocol, named cross resonance, which is theoretically treated in ref. 9 for a pair of qubits linearly coupled by a circuit element. Our system consists of two capacitively shunted flux qubits (CSFQs) which are coupled dispersively through the cavity, and the two-qubit interaction is tuned via the application of microwaves on individual qubit bias lines. We find that the two-qubit interaction turns on linearly with the amplitude of the applied CR drive, in which microwaves resonant with a target qubit are applied on the other control qubit. Up to single-qubit rotations, the CR gate is related to the canonical controlled-not (CNOT), and we use it to generate non-classical states in the Bell basis. We find an optimal gate time of 220 ns at which we generate the maximum concurrence for our two-qubit states and a two-qubit gate fidelity of 80%.

CSFQs are a germane choice for testing the CR protocol, since they have been shown to give consistently long coherence times in a circuit QED scheme[11]. Figures 1a-b show the schematic of our experimental setup and optical images of our sample, in which two CSFQs are coupled to opposite ends of a coplanar-waveguide resonator ($\omega_{\rm R}/2\pi = 9.72\,{\rm GHz}$) and on-chip flux bias lines (FBLs) are used to independently tune them to their flux sweet-spot transition energies, $\omega_1/2\pi = 5.854\,{\rm GHz}$ and $\omega_2/2\pi = 5.528\,{\rm GHz}$. Here, we find optimal relaxation and decoherence times for both CSFQs, all in excess of $1.5\,\mu{\rm s}$. The CSFQ-resonator coupling is inferred to be

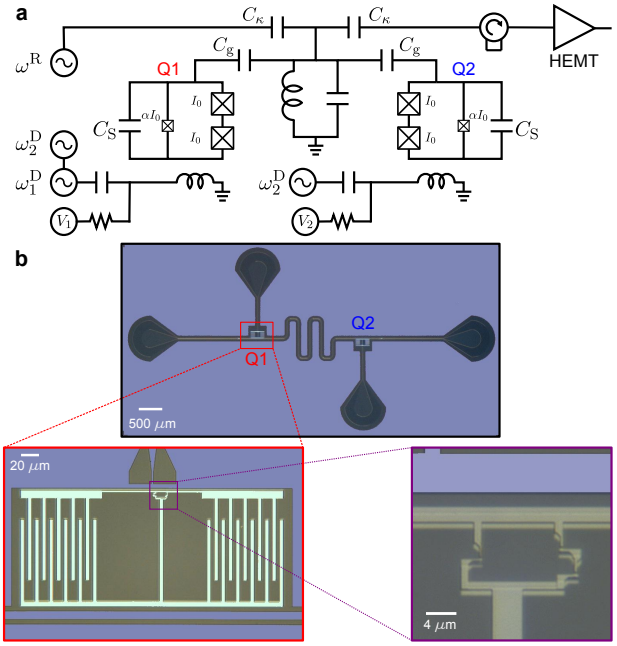

Figure 1. Circuit schematic and two-qubit device. **a**, Circuit schematic showing two CSFQ (Q1, red on left and Q2, blue on right) with shunt capacitance C_S and small junction ratio α, coupled to a single resonator. The qubit-cavity coupling is governed by C_g. Each CSFQ has an on-chip local flux-bias line which is used to both dc tune the energy levels and serve as a microwave excitation port for driving transitions. A joint two-qubit readout is performed by probing the system through the input port near the cavity frequency and detecting the transmission from the output port. **b**, Optical micrographs of actual device (false-colored), where the resonator is realized as a coplanar waveguide with measured frequency $\omega_R = 9.72\,\text{GHz}$ and linewidth $\kappa/2\pi = 1\,\text{MHz}$. When the qubits are near resonance with the cavity, the vacuum Rabi coupling strengths are found to be $g_{1,2}/\pi = 160\,\text{MHz}$. The flux-bias lines are terminated with an inductance to ground, off-centered from each qubit-loop.

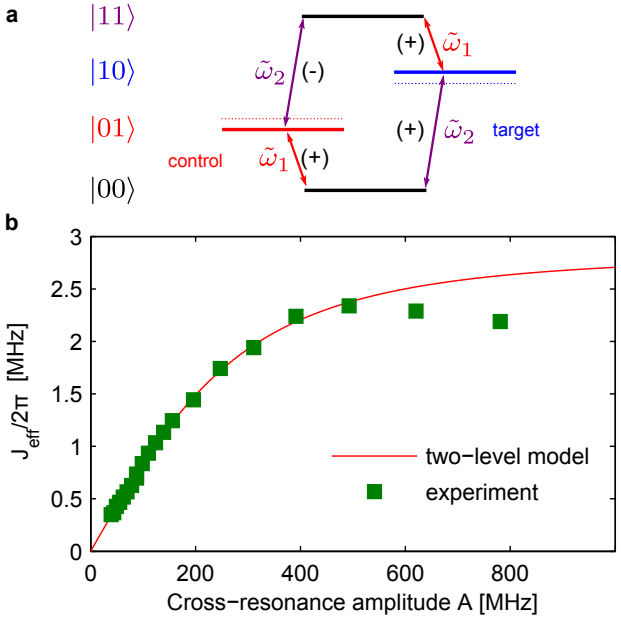

Figure 2. Cross-resonance level diagram and experimentally extracted tunable coupling strength. **a**, Energy spectrum corresponding to a pair of fixed weakly-coupled qubits ($\Delta_{12} > J$). Assuming qubit 1 as the control qubit, a cross-drive at the qubit 2 transition frequency rotates qubit 2, the target, with a phase dependent on the state of the control, with a rate down by a factor J/Δ_{12} over a resonant drive. **b**, The effective interaction strength for different cross-drive powers is found from the extracted frequency shift of the $\Omega_{R,2}$ with qubit 1 in either the ground or excited state. The interaction turns on linearly with the amplitude A of the drive, here shown normalized to $\Omega_{R,2}$, before leveling off at higher amplitudes when $\Omega_{R,2}$ approaches Δ_{12}.

$g_1/\pi = g_2/\pi = 160\,\text{MHz}$, with measured cavity shifts $2\chi_1 = 1.1\,\text{MHz}$ and $2\chi_2 = 0.6\,\text{MHz}$ permitting a joint two-qubit readout[21,22]. Gaussians with quadrature derivative pulse-shaping are used for single-qubit gates[23], $U_i(\theta)$ where $U = X, Y$, $i = 1, 2$ indexes the qubits, and θ the rotation angle, which are applied directly on each qubit's FBL.

The key for implementing the CR scheme on our sample is to apply microwave excitations resonant with the opposite qubit's transition frequency directly onto either qubit via the FBLs (figure 1a). To understand how the CR effect arises, consider the hamiltonian for a pair of qubits which are detuned from the resonator by $\Delta_i = \omega_i - \omega_R$ for $i = 1, 2$, and dispersively coupled to each other via the resonator,

$$H = \frac{1}{2}\omega_1\sigma_{z,1} + \frac{1}{2}\omega_2\sigma_{z,2} + J\left(\sigma_{+,1}\sigma_{-,2} + \sigma_{+,2}\sigma_{-,1}\right), \quad (1)$$

where $\sigma_{z,i}$ is a Pauli z matrix for qubit i and $J = g_1 g_2(1/\Delta_1 + 1/\Delta_2)$ is the fixed virtual qubit-qubit interaction[19]. Equation 1 can be diagonalized and considered as a new set of two qubits with shifted frequencies $\tilde{\omega}_1 = \omega_1 - J/\Delta_{12}$, $\tilde{\omega}_2 = \omega_2 + J/\Delta_{12}$ when J is small compared to the qubit-qubit detuning, $\Delta_{12} = \omega_1 - \omega_2$ (see figure 2a). In this frame, a single drive on qubit 1 at either $\tilde{\omega}_1$ or $\tilde{\omega}_2$ can excite transitions to qubit 1 or 2, respectively. However, the CR drive amplitude of qubit 2 is reduced by a factor of J/Δ_{12} and acquires a phase which is dependent on the state of qubit 1. The drive hamiltonian then takes the form

$$H_D = \epsilon(t)\left(\sigma_{x,1} + \frac{J}{\Delta_{12}}\sigma_{z,1}\sigma_{x,2}\right), \quad (2)$$

where $\epsilon(t)$ is the control on the drive. Hence, a drive on qubit 1 at $\tilde{\omega}_2$ can be used to turn on a ZX interaction, a primitive for a two-qubit CNOT[8]. The same analysis holds symmetrically for a drive applied to qubit 2. We will use the notation $\text{CR}_{ij}(A, t_g)$ to represent a cross drive on qubit i at ω_j with amplitude A and gate time t_g.

Although a ZX interaction theoretically corresponds to a change in phase of a qubit 2 rotation dependent

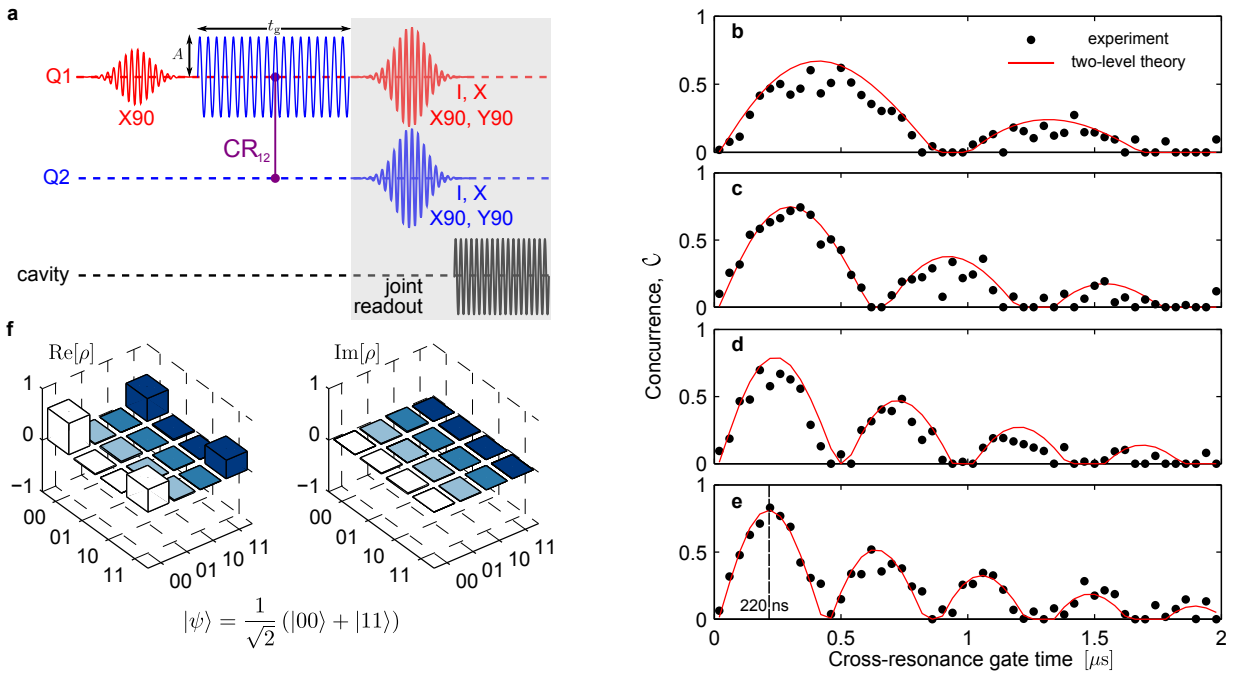

Figure 3. Entangled states and concurrence oscillations.**a**, Pulse sequence for generating entangled states; qubit 1 is first placed into a superposition state with a $R_{x,1}(\pi/2)$, leaving the system in the separable state $|\psi\rangle = (|00\rangle + |10\rangle)/\sqrt{2}$; next the CR_{12} pulse is also applied to qubit 1 before the joint readout sequence. The concurrence can be computed for all density matrices obtained with this pulse protocol, and oscillations are observed as a function of the gate time t_g for four different CR_{12} drive amplitudes **b-e**, corresponding to $\{X1, X2, X3, X4\}$ MHz. The period of the oscillations correspond to $1/J_{\rm eff}$ and the maximum concurrence is observe at $t_g = 220$ ns at $A = X4$. **f**, Measured density matrix for Bell-state $|\psi_{\rm Bell}\rangle = (|00\rangle + |11\rangle)/\sqrt{2}$ generated at the point of optimal concurrence labeled in **e**.

on the qubit 1 state, in practice due to spurious crosstalk resulting from stray electromagnetic coupling in the sample circuit and package[24], CR_{12} also directly induces rotations of qubit 2. As discussed in ref. 9, this does not demerit the two-qubit interaction. Rather, the effective interaction strength $J_{\rm eff}$ is simply manifested as the difference in qubit 2 Rabi oscillation frequencies ($\Omega_{\rm R,2}$) dependent on the state of qubit 1.

Figure 2b shows the experimentally measured $J_{\rm eff}$ versus A. We shape the CR_{12} pulse as a slow gaussian turn-on with a flat-top and a derivative-pulse correction on the quadrature (see Methods). With and without a single qubit $X_1(180)$ gate on qubit 1, we find different $\Omega_{\rm R,2}$, extracted from oscillations of the qubit 2 excited state population versus the time of the CR_{12} pulse t_g. For small A, $J_{\rm eff}$ turns on linearly. However, at stronger drives, the interaction strength levels off to a maximum of 2.6 MHz. This is in agreement with a two-level theory[9] and is due to the off-resonant driving of $\sigma_{x,1}$ in eq. 2.

Non-classical states can be generated and measured using the protocol in figure 3a, in which a $X_1(90)$ gate creates a superposition state of the control qubit, followed by the CR_{12} gate before the joint readout is used to perform state tomography and reconstruct the two-qubit density matrix ρ. The joint readout consists of 15 different single-qubit operations right before the measurement, from which ρ can be extracted using maximum-likelihood estimation. Although the joint readout scheme is not sensitive to excess mixtures of the two-qubit identity in the density matrix, we make the assumption that the qubits start in a pure state given the system temperature of 15 mK.

A standard metric of entanglement, the concurrence $\mathcal{C}$, can be computed for two-qubit states generated with the protocol for different t_g and A. Figures 3b–e show the evolution of $\mathcal{C}$ with t_g for four different A. We find that $\mathcal{C}$ oscillates with a period of with $1/J_{\rm eff}$. The points of maximal concurrence correspond to $t_g = 1/2J_{\rm eff}$, where the CR_{12} is a $[ZX]^{1/2}$ two-qubit operation which generates maximally entangled states in the Bell basis. The solid lines in fig. 3b–e correspond to master-equation two-level simulations taking into account the gate and coherence times.

In fig. 3f we show a measured ρ for one of the maximally entangled Bell basis states $|\psi_{\rm Bell}\rangle = 1/\sqrt{2}(|00\rangle + |11\rangle)$, generated with a CR_{12} gate at $t_g = 220$ ns and the amplitude A which gives the maximal $J_{\rm eff}$ in fig. 2b. Due to the spurious crosstalk on qubit 2 during the gate, an additional single qubit rotation of qubit 2 is usually performed. Although this extra rotation can be simply un-done with an additional single-qubit gate, for this specific t_g, the additional rotation from the crosstalk is $X_2(90)$, which

when combined with the $[ZX]^{1/2}$ leaves the two qubits in the canonical Bell state $|\psi_{\rm Bell}\rangle$. The fidelity to the ideal $|\psi_{\rm Bell}\rangle$ is found to be $\mathcal{F} = \langle\psi_{\rm Bell}|\rho|\psi_{\rm Bell}\rangle = 90\% \pm 0.04$ with a concurrence of $\mathcal{C} = 0.88 \pm 0.05$.

The $\rm CR_{12}$ gate is finally characterized using Quantum Process Tomography (QPT). First, we create the input states corresponding to combinations of $\{I, X_i(\pm 90), Y_i(\pm 90), X_i(\pm 180)\}$ on both qubits. Then we operate $\rm CR_{12}(A, t_g)$ on all 36 such input states and perform state tomography. The process matrix χ is obtained and compared to the ideal $\chi_{\rm ideal}$ (see fig. 4) to give a process fidelity $\mathcal{F}_p = 0.77$ and a gate fidelity[25] $\mathcal{F}_{\rm g} = 0.81$. The ideal gate fidelity taking into account the gate and coherence times is 0.86. As a measure of the effectiveness of our gate we also perform QPT for a 220 ns identity operation and we find $\mathcal{F}_{\rm g} = 0.81$ and $\mathcal{C} = 0.09$, which is consistent with a measured residual ZZ interaction of 200 kHz[4].

Thus, we have developed a microwaves-only scheme for a two-qubit universal gate capable of generating highly entangled states with superconducting qubits. Furthermore, the underlying two-qubit interaction is tunable simply via increasing the amplitude of a microwave drive. Although we saturate to a maximal interaction strength in this work (fig. 2b), we anticipate surpassing this limit with additional pulse shaping on the cross-resonance drive in the future. The tunable coupling protocol is simple to implement and requires no additional subcircuits or controls other than those for addressing each qubit independently. Expanding to more than two qubits should be very straightforward and will allow for the coupling of non-nearest neighbour qubits in frequency. The cross-resonance protocol could become a useful scheme for larger scale quantum information processors.

METHODS

SAMPLE FABRICATION

The device is fabricated on a 720 μm thick silicon substrate. The superconducting transmission-line cavity and flux-bias lines are defined via optical lithography and fluorine-based reactive ion etching of a dc-sputtered niobium film (180 nm thick). The two CSFQs are patterned using electron-beam lithography, grown using double-angle deposition of aluminium, with layer thicknesses of XX nm and XX nm. The sample is cooled in a dilution refrigerator to 15 mK.

EXPERIMENTAL DEVICE PARAMETERS

From a set of heterodyne transmission measurements obtained when tuning each CSFQ near resonance with the CPW resonator, we determine the CSFQ-resonator coupling strengths $g_{\rm L(R)}/2\pi = 160\,(160)$ MHz. DC flux bias is applied to both CSFQs, tuning them to their respective flux sweet-spots, where relaxation times are $T_1^{1(2)} = 2.5\,(1.5)\,\mu$s and dephasing times are $T_2^{1(2)} = 2.5\,(1.5)\,\mu$s. The CSFQ anharmonicities are measured to be $\alpha_1 = \omega_1^{12} - \omega_1^{01} = 224$ MHz and $\alpha_2 = \omega_2^{12} - \omega_2^{01} = 255$ MHz.

PULSE-SHAPING AND JOINT READOUT

Gaussian pulse shapes are used for x and y single-qubit rotations with $\sigma = 4$ ns and total gate length 4σ, with derivative-gasusian shapes on the quadrature for minimizing leakage errors[22,23]. The scale parameter for the derivative-gasussians[2] are experimentally determined to be -1.4 for both qubits. The joint readout assumes the measurement ensemble to be $\langle M\rangle = \beta_{IZ}\langle IZ\rangle + \beta_{ZI}\langle ZI\rangle + \beta_{ZZ}\langle ZZ\rangle$. Calibration of the readout gives $[\beta_{IZ}, \beta_{ZI}, \beta_{ZZ}] = [1, 0.9, 0.65]$. The $\rm CR_{12}$ pulse is also shaped with a gaussian ($\sigma = 10$ ns) turn-on to square top and derivative shape (scale parameter of -0.8) for the quadrature. For the QPT, the 36 input states generate an overcomplete set of measurements, from which χ is obtained using standard least-squares estimation.

1. Lucero, E. *et al.* High-fidelity gates in a single Josephson qubit. *Phys. Rev. Lett.* **100**, 247001 (2008).
2. Chow, J. M. *et al.* Optimized driving of superconducting artificial atoms for improved single-qubit gates. *Phys. Rev. A* **82**, 040305–040305 (2010). URL `http://link.aps.org/doi/10.1103/PhysRevA.82.040305`.
3. Plantenberg, J. H., de Groot, P. C., Harmans, C. J. P. M. & Mooij, J. E. Demonstration of controlled-not quantum gates on a pair of superconducting quantum bits. *Nature* **447**, 836–839 (2007).
4. DiCarlo, L. *et al.* Demonstration of two-qubit algorithms with a superconducting quantum processor. *Nature* **460**, 240–244 (2009).
5. Ansmann, M. *et al.* Violation of Bell's inequality in Josephson phase qubits. *Nature* **461**, 504–506 (2009).
6. DiCarlo, L. *et al.* Preparation and measurement of three-qubit entanglement in a superconducting circuit. *Nature* **467**, 574–578 (2010). URL `http://dx.doi.org/10.1038/nature09416`.
7. Neeley, M. *et al.* Generation of three-qubit entangled states using superconducting phase qubits. *Nature* **467**, 570–573 (2010). URL `http://dx.doi.org/10.1038/nature09418`.
8. Paraoanu, G. S. Microwave-induced coupling of superconducting qubits. *Phys. Rev. B* **74**, 140504–140504 (2006). URL `http://link.aps.org/doi/10.1103/PhysRevB.74.140504`.
9. Rigetti, C. & Devoret, M. Fully microwave-tunable universal gates in superconducting qubits with linear couplings and fixed transition frequencies. *Phys. Rev. B* **81**, 134507–134507 (2010). URL `http://link.aps.org/doi/10.1103/PhysRevB.81.134507`.
10. de Groot, P. C. *et al.* Selective darkening of degenerate transitions demonstrated with two superconducting quantum bits. *Nat Phys* **6**, 763–766 (2010). URL `http://dx.doi.org/10.1038/nphys1733`.
11. Steffen, M. *et al.* High-coherence hybrid superconducting qubit. *Phys. Rev. Lett.* **105**, 100502–100502 (2010). URL `http://link.aps.org/doi/10.1103/PhysRevLett.`

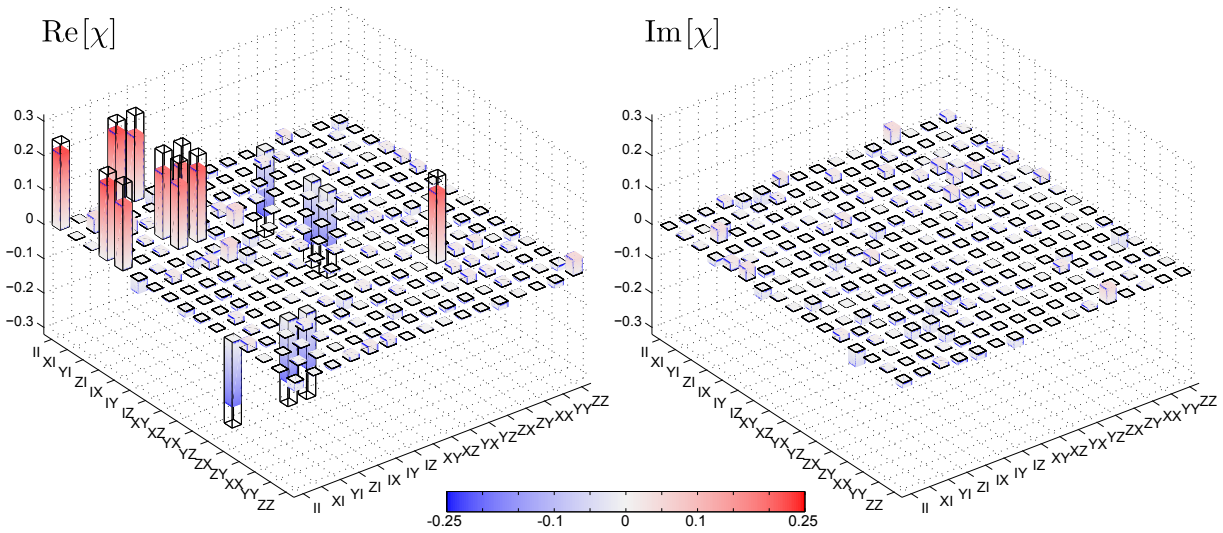

Figure 4. Quantum process tomography. Re[χ] and Im[χ] for the optimal CR_{12} gate are shown as the colored bars, corresponding to $t_{\text{gate}} = 220\,\text{ns}$ and A'. The ideal two-qubit gate corresponds to a CNOT two-qubit unitary, and the corresponding Re[χ_{ideal}] and Im[χ_{ideal}] are shown as the transparent bars. All Im[χ] bars are < 0.05.

105.100502.

12. Bertet, P., Harmans, C. J. P. M. & Mooij, J. E. Parametric coupling for superconducting qubits. *Phys. Rev. B* **73**, 064512–064512 (2006). URL `http://link.aps.org/doi/10.1103/PhysRevB.73.064512`.
13. Niskanen, A. O. *et al.* Quantum coherent tunable coupling of superconducting qubits. *Science* **316**, 723–726 (2007).
14. Harris, R. *et al.* Sign- and magnitude-tunable coupler for superconducting flux qubits. *Phys. Rev. Lett.* **98**, 177001–177001 (2007). URL `http://link.aps.org/doi/10.1103/PhysRevLett.98.177001`.
15. Hime, T. *et al.* Solid-state qubits with current-controlled coupling. *Science* **314**, 1427–1429 (2006).
16. Bialczak, R. C. *et al.* Fast tunable coupler for superconducting qubits. *Phys. Rev. Lett.* **106**, 060501–060501 (2011). URL `http://link.aps.org/doi/10.1103/PhysRevLett.106.060501`.
17. Steffen, M. *et al.* Measurement of the entanglement of two superconducting qubits via state tomography. *Science* **313**, 1423–1425 (2006).
18. Bialczak, R. C. *et al.* Quantum process tomography of a universal entangling gate implemented with josephson phase qubits. *Nat Phys* **6**, 409–413 (2010). URL `http://dx.doi.org/10.1038/nphys1639`.
19. Majer, J. *et al.* Coupling superconducting qubits via a cavity bus. *Nature* **449**, 443–447 (2007).
20. Sillanpää, M. A., Park, J. I. & Simmonds, R. W. Coherent quantum state storage and transfer between two phase qubits via a resonant cavity. *Nature* **449**, 438–442 (2007).
21. Filipp, S. *et al.* Two-qubit state tomography using a joint dispersive readout. *Phys. Rev. Lett.* **102**, 200402 (2009).
22. Chow, J. M. *et al.* Detecting highly entangled states with a joint qubit readout. *Phys. Rev. A* **81**, 062325–062325 (2010). URL `http://link.aps.org/doi/10.1103/PhysRevA.81.062325`.
23. Motzoi, F., Gambetta, J. M., Rebentrost, P. & Wilhelm, F. K. Simple pulses for elimination of leakage in weakly nonlinear qubits. *Physical Review Letters* **103**, 110501–4 (2009).
24. Wenner, J. *et al.* Wirebond crosstalk and cavity modes in large chip mounts for superconducting qubits. *Supercond. Sci. Technol.* **24**, 065001–065001 (2011). URL `http://iopscience.iop.org/0953-2048/24/6/065001`.
25. Nielsen, M. A. A simple formula for the average gate fidelity of a quantum dynamical operation. *Phys. Lett. A* **303**, 249–252 (2002).

Acknowledgements We thank Kent Fung and Jack Rohrs for experimental contributions and M. Silva for engaging theoretical discussions. We acknowledge support from IARPA under contract XXXXXXX. All statements of fact, opinion or conclusions contained herein are those of the authors and should not be construed as representing the official views or policies of the U.S. Government.

Author contributions J.M.C designed and performed the experiments. J.M.C., A.D.C, J.M.G., and M.S. interpreted and analyzed the experimental data. J.M.G., C.R, J.A.S. provided theoretical support. J.M.C. and B.R.J. developed control hardware and software. J.R., G.A.K, M.B.R fabricated samples. All authors contributed to the composition of the manuscript.